Acta Crystallographica Section F
Structural Biology and Crystallization Communications
ISSN 1744-3091

Crystallization and preliminary crystallographic analysis of DtsR1, a carboxyltransferase subunit of acetyl-CoA carboxylase from *Corynebacterium glutamicum*

Minoru Yamada,[a,b] Ryo Natsume,[b] Tsuyoshi Nakamatsu,[a] Sueharu Horinouchi,[c] Hisashi Kawasaki[a] and Toshiya Senda[d]*

[a]Materials Science and Engineering, Graduate School of Engineering, Tokyo Denki University, 2-2 Nishiki-cho, Kanda, Chiyoda-ku, Tokyo 101-8457, Japan, [b]Japan Biological Information Research Center, Japan Biological Informatics Consortium, 2-42 Aomi, Koto-ku, Tokyo 135-0064, Japan, [c]Department of Biotechnology, Graduate School of Agriculture and Life Sciences, The University of Tokyo, 1-1-1 Yayoi, Bunkyo-ku, Tokyo 113-8657, Japan, and [d]Biological Information Research Center, National Institute of Advanced Industrial Science and Technology, 2-42 Aomi, Koto-ku, Tokyo 135-0064, Japan

Correspondence e-mail: tsenda@jbirc.aist.go.jp

Received 16 October 2006
Accepted 9 January 2007

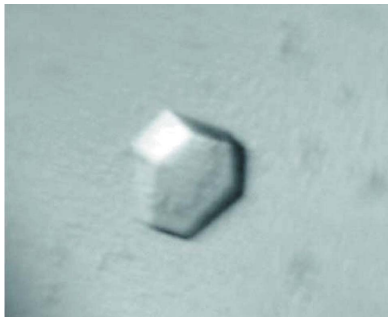

DtsR1, a carboxyltransferase subunit of acetyl-CoA carboxylase derived from *Corynebacterium glutamicum*, was crystallized by the sitting-drop vapour-diffusion method using polyethylene glycol 6000 as a precipitant. The crystal belongs to the trigonal system with space group *R*32 and contains three subunits in the asymmetric unit. A molecular-replacement solution was found using the structure of transcarboxylase 12S from *Propionibacterium shermanii* as a search model.

1. Introduction

Corynebacterium glutamicum is a Gram-positive and biotin-auxotroph bacterium that has long been used industrially to produce glutamate (Hermann, 2003). Glutamate overproduction in *C. glutamicum* is induced by the depletion of biotin (Shiio *et al.*, 1962), the addition of a specific detergent such as polyoxyethylene sorbitan monopalmitate (Tween 40; Takinami *et al.*, 1965) or the addition of a sublethal concentration of penicillin (Nunheimer *et al.*, 1970). A recent study showed that the activity of the 2-oxoglutarate dehydrogenase complex (ODHC; EC 1.2.4.2) is reduced under each of these conditions (Shingu & Terui, 1971; Kawahara *et al.*, 1997), leading to an increase in the carbon flow towards glutamate synthesis at the ODHC branch point (Shimizu *et al.*, 2003). However, the molecular mechanism underlying glutamate overproduction remains elusive.

DtsR1 was identified as a suppresser gene for a Tween 40-sensitive mutant strain that is more sensitive to Tween 40 for glutamate production than the wild type (Kimura *et al.*, 1996). Genetic and biochemical studies showed that *dtsR1* encodes the carboxyltransferase subunit (CT) of the acetyl-CoA carboxylase complex (ACC; EC 6.4.1.2), which catalyzes the first committed step in fatty-acid biosynthesis (Kimura *et al.*, 1997; Gande *et al.*, 2004). It was observed that disruption of *dtsR1* causes a reduction in ODHC activity, resulting in constitutive glutamate production in the absence of inducers (Kimura *et al.*, 1997). In addition, overexpression of *dtsR1* inhibits glutamate production (Kimura *et al.*, 1999). These studies suggested that a functional (and probably physical) interaction between DtsR1 and ODHC is involved in glutamate production and that a reduction in DtsR1 activity triggers a reduction in ODHC activity, enhancing the glutamate synthesis from 2-oxoglutarate (Kimura *et al.*, 1999). Therefore, DtsR1 is considered as a potential target for metabolic engineering to improve glutamate overproduction in *C. glutamicum*. Towards this end, knowledge of the structure–function relationship of DtsR1 is required.

Several crystal structures of bacterial CT homologues and eukaryotic CT domains have already been determined: those of transcarboxylase 12S from *Propionibacterium shermanii* (Hall *et al.*, 2003), a CT of the sodium ion pump glutaconyl-CoA decarboxylase from *Acidaminococcus fermentans* (Gcdα; Wendt *et al.*, 2003), a CT of propionyl-CoA carboxylase from *Streptomyces coelicolor* A3(2) (*Sc*PCCB; Diacovich *et al.*, 2004), a CT of acyl-CoA carboxylase from *Mycobacterium tuberculosis* (*Mt*AccD5; Lin *et al.*, 2006), the CTs of ACC from *Staphylococcus aureus* (*Sa*CT) and *Escherichia coli* (*Ec*CT; Bilder *et al.*, 2006) and a CT domain of ACC from *Saccharomyces cerevisiae* (yeast-CT; Zhang *et al.*, 2003). The typical CT subunit is composed of two repetitions of a crotonase-fold domain.

Table 1
Summary of data collection.

Values in parentheses are for the highest shell.

Data set	I	II
Beamline	PF-AR NW12	PF BL5
Wavelength (Å)	1.0	1.13
Detector	ADSC Quantum 210	ADSC Quantum 315
Space group	*R*32	*R*32
Unit-cell parameters (Å)		
$a = b$	204.21	203.67
c	234.02	233.67
Resolution (Å)	48.8–3.20 (3.37–3.20)	48.7–2.60 (2.74–2.60)
$R_{\rm merge}$† (%)	9.9 (43.7)	8.8 (41.9)
$I/\sigma(I)$	14.6 (4.2)	15.5 (4.0)
No. of measured reflections	224323	404804
No. of unique reflections	31055	57152
Completeness (%)	100 (100)	100 (100)
Multiplicity	7.2 (7.3)	7.1 (7.2)

† $R_{\rm merge} = \sum_h \sum_i |I(h) - I(h)_i| / \sum_h [N \times I(h)]$.

Although the structures of these CTs are similar to one another, with root-mean-square deviations in the range 0.79–1.91 Å, the surface residues of these CTs, which include the substrate-binding site and its peripheral region, are not well conserved. These differences seem to be important for substrate-specificity and interaction with specific biotinoyl carboxyl carrier proteins. DtsR1 shows 48.4, 20.9, 57.8, 65.5, 19.1, 20.1 and 20.3% amino-acid identity with 12S, Gcdα, *Sc*PCCB, *Mt*AccD5, *Sa*CT, *Ec*CT and yeast-CT, respectively, suggesting that DtsR1 has essentially the same fold as related proteins. However, since the differences between DtsR1 and other related CTs, most of which are expected to be located on the surface of the DtsR1 molecule, are likely to be responsible for the substrate-specificity and species-specific interaction with biotinoyl carboxyl carrier protein, detailed structural information is still required in order to understand the structure–function relationship of DtsR1. Therefore, we initiated structural analysis of DtsR1 in order to understand the details of its structure–function relationship for use in metabolic engineering of *C. glutamicum*. Here, we report the overexpression, crystallization and preliminary crystallographic analysis of DtsR1.

2. Results and discussion

2.1. Protein expression and purification

The *dtsR1* gene was subcloned from a pUC19 plasmid carrying the *dtsR1* gene (unpublished data) into the pET26b(+) expression vector (Novagen) to produce DtsR1 with a histidine tag (SHHHHHH) at its C-terminus. *E. coli* BL21 (DE3) containing the expression vector was cultured at 299 K in 2 l LB medium containing 20 µg ml^{-1} kanamycin. Expression was induced by the addition of IPTG to a final concentration of 1.0 m*M* at a cell density of OD_{600} = 0.5–0.6. The cells were harvested by centrifugation after 3 h induction. The bacterial cell pellet was resuspended in 10 m*M* imidazole, 500 m*M* sodium chloride, 10%(*v*/*v*) glycerol, 50 m*M* sodium phosphate buffer pH 8.0 (buffer *A*) and homogenized by sonication. The lysate was centrifuged at 20 000*g* for 2 h to remove cell debris. The supernatant was applied onto a Chelating Sepharose FF column (50 ml, GE Healthcare) with immobilized Ni^{2+} previously equilibrated with buffer *A*. After the column had been washed with buffer *A* containing 50 m*M* imidazole, DtsR1 was eluted with a linear imidazole gradient (50–300 m*M*). SDS–PAGE analysis of the purified DtsR1 revealed a single band of 58 kDa, indicating that DtsR1 was purified to near-homogeneity. The purified DtsR1 was flash-frozen in liquid nitrogen and stored at 193 K. Prior to crystallization, an appropriate amount of DtsR1 was thawed and concentrated to approximately 20 mg ml^{-1} using an Amicon Ultra-15 membrane (Millipore) with a molecular-weight cutoff (MWCO) of 30 kDa. The concentrated protein was dialyzed twice against 50 m*M* sodium phosphate buffer pH 7.0 using Spectra/Por CE membrane tubing (Spectrum) with an MWCO of 8 kDa at 277 K for 2 h. The dialysate was again concentrated to approximately 15 mg ml^{-1} using a Centricon YM-30 (Millipore). Protein concentrations were estimated spectroscopically by measuring the A_{280}, assuming an A_{280} of 0.654 for a 1.0 mg ml^{-1} solution.

2.2. Crystallization

Initial crystallization screening was performed using the hanging-drop vapour-diffusion method with Crystal Screens I and II (Hampton Research) at 293 K. A hanging drop was prepared by mixing 2.0 µl each of the protein and reservoir solutions and was equilibrated against 0.5 ml reservoir solution. Crystals appeared under the following two conditions: (i) 0.2 *M* zinc acetate dihydrate, 0.1 *M* sodium cacodylate pH 6.5, 18%(*w*/*v*) polyethylene glycol (PEG) 8000 and (ii) 2 *M* sodium chloride and 10%(*w*/*v*) PEG 6000. A diffraction study using an R-AXIS IV^{++} detector (Rigaku) mounted on an FR-D rotating-anode X-ray generator (Rigaku) showed that only the latter crystals diffracted (to approximately 7 Å resolution). The crystallization conditions were optimized by systematically varying the concentrations of protein, PEG 6000 and sodium chloride. Since the sitting-drop vapour-diffusion method yielded larger DtsR1 crystals than the hanging-drop method, we chose the sitting-drop vapour-diffusion method for the optimization. The best crystal was obtained from a sitting drop prepared by mixing 4.5 µl each of the protein and reservoir solutions and equilibrated against 0.5 ml reservoir solution. The reservoir condition was 2.0 *M* sodium chloride and 9.25–9.75%(*w*/*v*) PEG 6000. The protein was at 14 mg ml^{-1} in 50 m*M* sodium phosphate buffer pH 7.0. DtsR1 aggregated immediately after being mixed with the reservoir solution. Crystals only grew from the drops with aggregation. The crystal growth was sensitive to the concentration of PEG 6000; a 0.5% difference affected the size of the crystals. Hexagonal crystals grew to average dimensions of 0.08 × 0.08 × 0.03 mm in two weeks (Fig. 1).

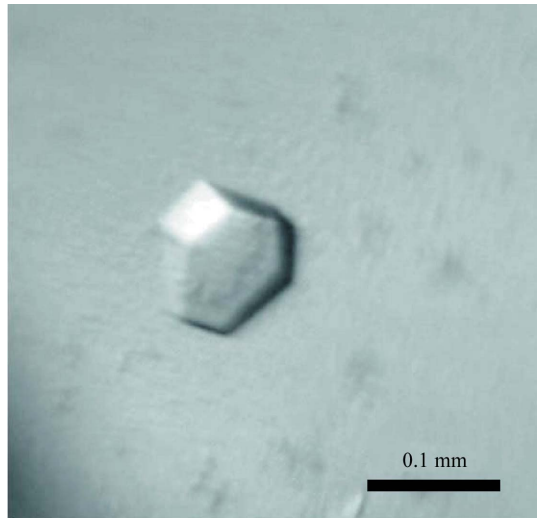

Figure 1
Crystal of DtsR1.

2.3. Data collection and processing

Data collections were carried out using synchrotron radiation at Photon Factory (PF, Tsukuba). The crystals were soaked in cryoprotectant solution [15%(*w*/*v*) PEG 6000, 2.0 *M* sodium chloride, 0.05 *M* sodium phosphate buffer pH 7.0] for a few seconds and flash-frozen at 100 K in a cold N_2 stream from a liquid-nitrogen cryostat (Rigaku). Two sets of diffraction data, data sets I and II, were collected using an ADSC CCD detector (Table 1). Each data set was processed using *MOSFLM* (Leslie, 1992) and scaled with *SCALA* from the *CCP*4 program suite (Collaborative Computational Project, Number 4, 1994; Table 1). The two crystals used for data collection were isomorphous and belonged to the trigonal system, with space group *R*32. Assuming the asymmetric unit to contain three subunits, we calculated the V_M value (Matthews, 1968) for both data sets I and II as 2.6 Å^3 Da^{-1}. The corresponding solvent content was approximately 53%. Threefold noncrystallographic symmetry could not be found in a Patterson self-rotation map calculated using *POLARRFN* from the *CCP*4 program suite (Collaborative Computational Project, Number 4, 1994). Data set I was used for molecular-replacement calculations and data set II was used for crystallographic refinement.

2.4. Molecular replacement

Molecular replacement was performed with *MOLREP* (Vagin & Teplyakov, 1997) from the *CCP*4 program suite using data set I (Table 1). The coordinates of the *A* subunit of transcarboxylase 12S from *P. shermanii* (PDB code 1on3; Hall *et al.*, 2003), which shows 48.4% amino-acid sequence identity to DtsR1, was used as a search model. Because there were no significant peaks in the cross-rotation function, translation functions were calculated for each of the first 30 peaks of the rotation function. We were able to find three subunits in the asymmetric unit without unfavourable molecular contacts in the crystal lattice. After a few cycles of rigid-body and simulated-annealing refinement at 3.2 Å resolution using *CNS* (Brünger *et al.*, 1998), the R_{work} and R_{free} factors fell to 29.5% and 35.5%, respectively, suggesting that the obtained model was a correct solution. The results of molecular replacement suggest that DtsR1 is a ring-shaped homohexamer with 32 point-group symmetry, as found in other related proteins (Hall *et al.*, 2003; Diacovich *et al.*, 2004; Lin *et al.*, 2006). One subunit in the asymmetric unit forms a hexamer with its symmetry mates. The other two subunits in the asymmetric unit form another hexamer with their symmetry mates. The three subunits in the asymmetric unit are not related to one another by a noncrystallographic threefold axis, which is consistent with the Patterson self-rotation map. Further model building and crystallographic refinement at 2.6 Å resolution is in progress using data set II (Table 1). The R_{work} and R_{free} factors of the present model are 23.1% and 28.2%, respectively.

This work was partly supported by the Japan New Energy and Industrial Technology Development Organization (NEDO), Japan.

References

Bilder, P., Lightle, S., Bainbridge, G., Ohren, J., Finzel, B., Sun, F., Holley, S., Al-Kassim, L., Spessard, C., Melnick, M., Newcomer, M. & Waldrop, G. L. (2006). *Biochemistry*, **45**, 1712–1722.

Brünger, A. T., Adams, P. D., Clore, G. M., DeLano, W. L., Gros, P., Grosse-Kunstleve, R. W., Jiang, J.-S., Kuszewski, J., Nilges, M., Pannu, N. S., Read, R. J., Rice, L. M., Simonson, T. & Warren, G. L. (1998). *Acta Cryst.* D**54**, 905–921.

Collaborative Computational Project, Number 4 (1994). *Acta Cryst.* D**50**, 760–763.

Diacovich, L., Mitchell, D. L., Pham, H., Gago, G., Melgar, M. M., Khosla, C., Gramajo, H. & Tsai, S. C. (2004). *Biochemistry*, **43**, 14027–14036.

Gande, R., Gibson, K. J., Brown, A. K., Krumbach, K., Dover, L. G., Sahm, H., Shioyama, S., Oikawa, T., Besra, G. S. & Eggeling, L. (2004). *J. Biol. Chem.* **279**, 44847–44857.

Hall, P. R., Wang, Y. F., Rivera-Hainaj, R. E., Zheng, X., Pustai-Carey, M., Carey, P. R. & Yee, V. C. (2003). *EMBO J.* **22**, 2334–2347.

Hermann, T. (2003). *J. Biotechnol.* **104**, 155–172.

Kawahara, Y., Takahashi-Fuke, K., Shimizu, E., Nakamatsu, T. & Nakamori, S. (1997). *Biosci. Biotechnol. Biochem.* **61**, 1109–1112.

Kimura, E., Abe, C., Kawahara, Y. & Nakamatsu, T. (1996). *Biosci. Biotechnol. Biochem.* **60**, 1565–1570.

Kimura, E., Abe, C., Kawahara, Y., Nakamatsu, T. & Tokuda, H. (1997). *Biochem. Biophys. Res. Commun.* **234**, 157–161.

Kimura, E., Yagoshi, C., Kawahara, Y., Ohsumi, T., Nakamatsu, T. & Tokuda, H. (1999). *Biosci. Biotechnol. Biochem.* **63**, 1274–1278.

Leslie, A. G. W. (1992). *Jnt CCP4/ESF–EACBM Newsl. Protein Crystallogr.* **26**.

Lin, T. W., Melgar, M. M., Kurth, D., Swamidass, S. J., Purdon, J., Tseng, T., Gago, G., Baldi, P., Gramajo, H. & Tsai, S. C. (2006). *Proc. Natl Acad. Sci. USA*, **103**, 3072–3077.

Matthews, B. W. (1968). *J. Mol. Biol.* **33**, 491–497.

Nunheimer, T. D., Birnbaum, J., Ihnen, E. D. & Demain, A. L. (1970). *Appl. Microbiol.* **20**, 215–217.

Shiio, I., Otsuka, S. I. & Takahashi, M. (1962). *J. Biochem. (Tokyo)*, **51**, 56–62.

Shimizu, H., Tanaka, H., Nakato, A., Nagahisa, K., Kimura, E. & Shioya, S. (2003). *Bioprocess Biosyst. Eng.* **25**, 291–298.

Shingu, H. & Terui, G. (1971). *J. Ferment. Technol.* **49**, 400–405.

Takinami, K., Yoshii, H., Tsuri, H. & Okada, H. (1965). *Agric. Biol. Chem.* **29**, 351–359.

Vagin, A. & Teplyakov, A. (1997). *J. Appl. Cryst.* **30**, 1022–1025.

Wendt, K. S., Schall, I., Huber, R., Buckel, W. & Jacob, U. (2003). *EMBO J.* **22**, 3493–3502.

Zhang, H., Yang, Z., Shen, Y. & Tong, L. (2003). *Science*, **299**, 2064–2067.